Monoanionic NSiN-type Ligands in Transition Metal Coordination Chemistry and Catalysis†

Francisco J. Fernández-Alvarez,*[a] Ralte Lalrempuia[a,b] and Luis A. Oro*[a,c]

(a) Departamento de Química Inorgánica-Instituto de Síntesis Química y Catálisis Homogénea (ISQCH), Universidad de Zaragoza – CSIC, Facultad de Ciencias 50009, Zaragoza – Spain. E-mail: paco@unizar.es, oro@unizar.es.

(b) University of Bergen, Department of Chemistry, Allégaten 41, N-5007 Bergen, Norway.

(c) Visiting Professor, Center of Research Excellence in Petroleum Refining & Petrochemicals, King Fahd University of Petroleum & Minerals, 31261 Dhahran - Saudi Arabia.

† *Dedicated to Prof. Pierre Braunstein on the occasion of his 70th birthday with our most sincere congratulations for his leadership and outstanding contributions to the field of Coordination Chemistry and Catalysis, and best wishes.*

Abstract

The number of late transition metal complexes bearing tridentate monoanionic silyl-based NSiN-type ligands has grown in the last few years. This review describes the synthetic methodologies that allow preparation of NSiN ligands precursors as well as the chemical and structural behavior of the transition metal complexes resulting from the reaction of these ligand precursors with different metallic starting materials. In addition, a description of the catalytic processes based on Rh- and Ir-NSiN catalysts so far reported is included. Moreover, an analysis of the chemistry of iridium complexes with different *fac*-κ^3-(*Si*,*N*,*N*)-NSiN ligands allows to conclude that the nature of the silyl group along with the donor ability of the nitrogen atoms at the NSiN ligands influence on the reactivity and potential catalytic activity of the respective complexes.

Keywords

NSiN ligands – Transition-metal NSiN complexes - Coordination chemistry - Homogeneous Catalysis - Si-H activation.

1 Introduction.

The activity and selectivity of a catalyst are closely related to the nature of the active site. In the context of transition-metal based homogeneous catalysis, there has been longstanding interest in tuning the electronic and steric properties of the metal coordination environment to improve the catalytic performance [1, 2]. Particularly, monoanionic tridentate LEL-type ligands —where E symbolizes a central carbanion or less commonly a central silyl group and L are two-electron σ-donor groups— have proven to be versatile ligands, which allow modulating the chemical behaviour of the active site. The central atom (E) and the peripheral donor groups (L) of such ligands are covalently linked by carbon- or functionalized-carbon chains. Thus, the ligand puckering of LEL-type ligands depends on the nature of the donor atoms, the atoms in the linker chains, and if the case on the exocyclic substituents [3-9]. In pseudooctahedral metal complexes, LEL-type ligands could be coordinated to the corresponding transition metal in different modes (Figure 1). Among them are transition metal complexes with LEL-type ligands in κ^3-meridional or κ^3-facial coordination modes.

In this regard, monoanionic tridentate LSiL-ligands with a central silyl group usually bind to the metal centers in κ^3-facial coordination mode (Figure 1). It should be noted that monoanionic *fac*-κ^3-(*Si*,*N*,*N*)-LSiL ligands could be considered as six or five electron donors in the ionic or covalent model, respectively [2]. From that point of view, *fac*-κ^3-(*Si*,*N*,*N*)-LSiL ligands could be related to η^5-cyclopentadienyl [2, 10] and κ^3-trispyrazolylborate [2, 11] ligands since the latter could also behave as monoanionic six (or five in the covalent model) electron donor ligands and occupy a face in pseudooctahedral complexes.

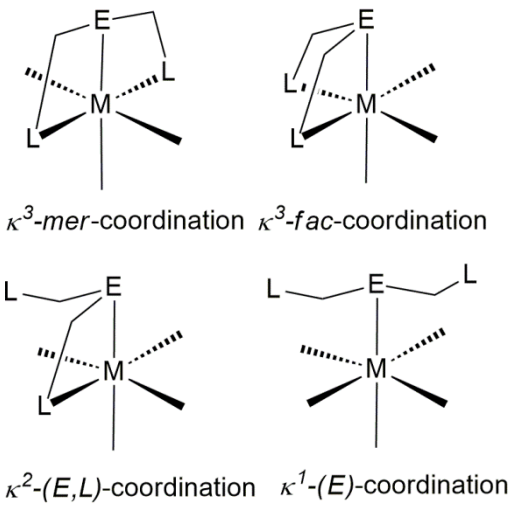

Figure 1. Examples of coordination modes for monoanionic LEL-type ligands in pseudooctahedral metal complexes (E = Csp^3, Csp^2, SiR; L = σ-donor ligand; M = transition metal).

A general feature of LSiL-ligands is that the presence of the central silyl-group favors the stabilization of high oxidation states on the resulting transition metal-complex and/or labilizes *trans* ligands due to the strong *trans* influence and *trans* effect of silyl groups [12]. The number of reports on transition metal complexes bearing LSiL-type ligands has grown considerably during the last decade. Among them are the phosphine based PSiP-metal species [8, 13, 14] pioneered by Stobart et al. [13h], whose chemistry has been widely explored. However, the related nitrogen based NSiN-metal complexes have been scarcely studied (Figure 2). Although, in recent years some remarkable contributions have been reported, which constitute the subject matter of this work.

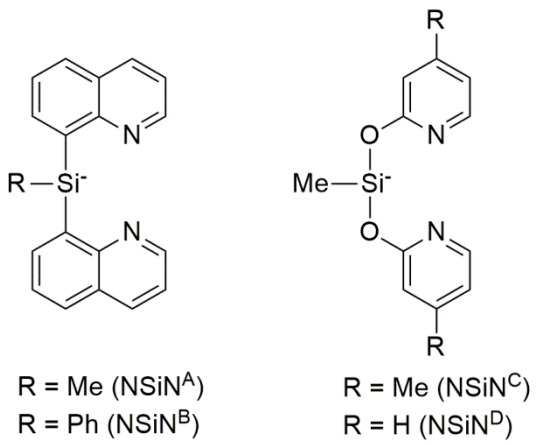

Figure 2. Examples of monoanionic tridentate NSiN ligands commonly used in transition metal coordination chemistry.

To the best of our knowledge the first examples of transition-metal derivatives with tridentate monoanionic NSiN-type ligands were reported by Tilley et al. in 2001, they prepared Ir-NSiN species with the ligand bis(8-quinolyl)methylsilyl ($NSiN^A$ in Figure 2) [15a]. This study opened the door to the chemistry of transition metal-NSiN complexes, which currently includes examples of Ir [15, 16], Rh [17, 18], Pt [19], Os [20] and Ni [21] species. In this contribution, we aimed to bring together a description of their structural characteristics and reactivity patterns as well as a rationalization of the electronic and steric factors that could determine the different activity of the catalytic systems based on NSiN-transition metal species.

2 Synthesis and characterization of transition metal NSiN-complexes

2.1. Synthesis of NSiN and related ligand precursors.

A general methodology for the synthesis of NSiN ligand precursors has been the treatment of the lithium salt of the corresponding N-heterocycle with an alkyl- or aryldichlorosilane (Scheme 1). Thus, dropwise addition of one equivalent of

$HSiCl_2Me$ to an in situ generated THF solution of 8-lithiumquinoline at -78ºC was found to be the best method for the preparation of bis-(8-quinolyl)methylsilane (**1**). This compound was isolated as a yellow crystalline solid in 48% (Equation 1, Scheme 1) [15a]. The related species, bis-(8-quinolyl)phenylsilane (**2**) was analogously prepared, and isolated as a yellow powder in 39% yield using $HSiCl_2Ph$ instead of $HSiCl_2Me$ (Equation 1, Scheme 1) [21].

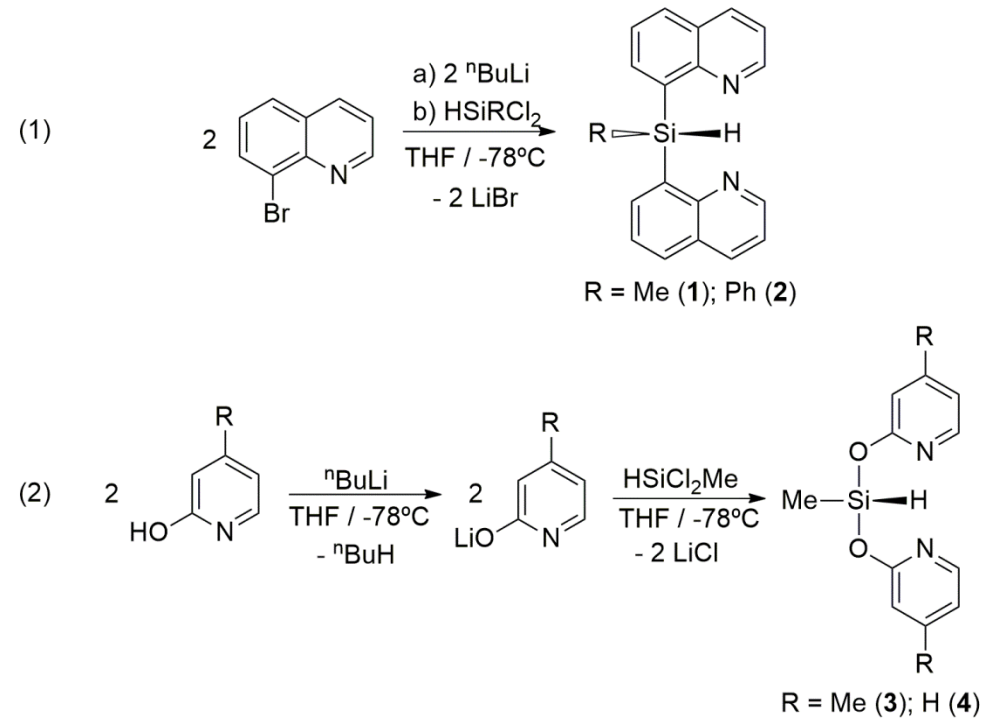

Scheme 1. Synthesis of NSiN ligand precursors.

The preparation of bis(pyridine-2-yloxy)methylsilane (**3**) [16a] and bis-(4-methylpyridine-2-yloxy)methylsilane (**4**) [16b] requires isolation and purification of the corresponding lithium pyridine-2-olate derivative prior to the subsequent step (Equation 2, Scheme 1). It is worth mentioning that the Si-O-C bonds in compounds **3** and **4** are highly sensitive to moisture and both compounds react quickly with traces of water to give the parent hydroxypyridine derivative and siloxanes. It should be noted that the $^{29}Si\{^1H\}$ NMR spectra of compounds **1**, **2**, **3** and **4** exhibit singlet

resonances in the high field region at δ -18.9, -23.8, -17.5 and -18.2 ppm, respectively.

On the other hand, Roper, Wright and co-authors reported a nice example of template synthesis of a pincer NSiN-ligand coordinated to osmium [20]. Treatment of [Os(Cl)($SiMeCl_2$)(PPh_3)$_2$(CO)] with two equivalents of 2-aminopyridine affords as major reaction product the osmium(II) complex [Os{*fac*-(κ^3(*Si,N,N´*)-SiMe(NH(2-C_5H_4N)$_2$)}(Cl)(CO)(PPh_3)] (**5**). The structure of **5** was determined by X-ray diffraction methods (Scheme 2) [20]. The Os-Si bond distance in complex **5** (2.3121(12) Å) is shorter than those commonly reported for osmium silyl derivatives (2.39−2.50 Å) [22]. The N-Os-N angle 84.1(1)º is slightly deviated from the octahedral geometry. In agreement with the strong *trans* influence exerted by the silyl group, a rather long Os-Cl bond distance 2.5503(11) Å was observed [20].

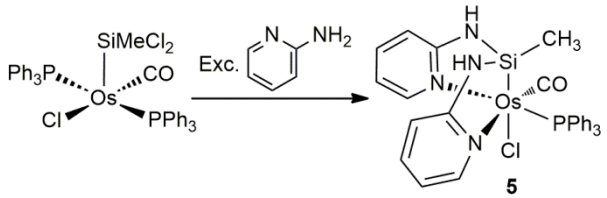

Scheme 2. Reaction of [Os(Cl)($SiMeCl_2$)(PPh_3)$_2$(CO)] with 2-aminopyridine.

A related example of template synthesis of an asymmetric *fac*-(κ^3(*Si,N,C*)-N-Si-NHC ligand coordinated to cobalt has been reported. Thus, dehydrogenative silylation of 2-pyridone with the Si-H bond present in the cobalt(II) complex **6** affords the Co-NSi-NHC species **7** (Scheme 3) [23a]. Interestingly, the chemical oxidation of **6** with [Cp_2Fe][BPh_4] affords the cobalt(III) species **8** with a *mer*-NHC-Si-NHC ligand (Scheme 3) [23b].

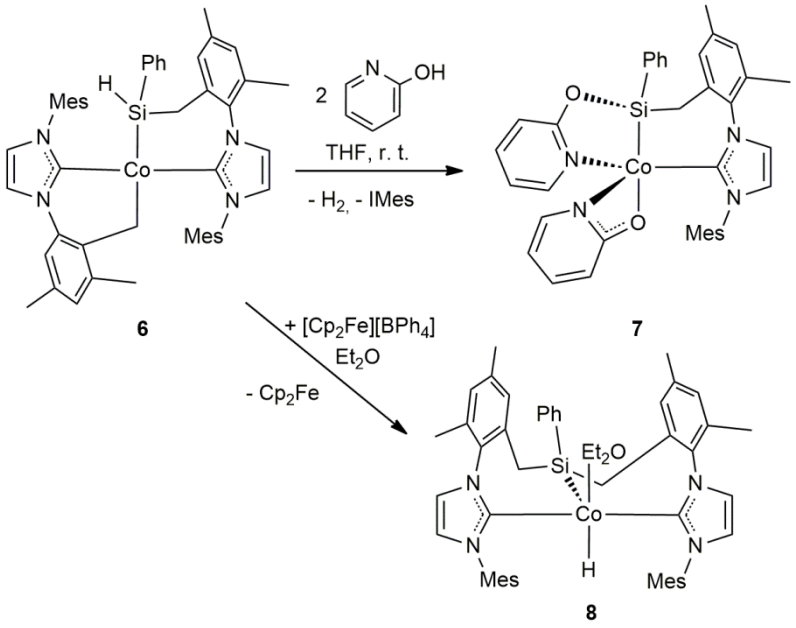

Scheme 3. Template synthesis of the cobalt(II) and cobalt(III) complexes **7** and **8**.

In this context, it should be mentioned that Turculet et al. have reported the reaction of compound [Si(H)(Me){2-^{t}BuP(C$_6$H$_4$)}{2-Me$_2$N(C$_6$H$_4$)}] (**9**) with the corresponding metallic starting material to afford the respective [M(H)(Cl){*mer*-κ^3(*Si*,*P*,*N*)-PSiN}] (M = Rh, Ir) or [M(X){*mer*-κ^3(*Si*,*P*,*N*)-PSiN}] (M = Pd, X = Br, TfO; Pt; X = Cl; TfO) complexes (Scheme 4) [24]. The amino group of the PSiN ligand in complexes **10**-**15** is labile and could be displaced from the metal coordination sphere by a stronger donor, such as PMe$_3$ [24].

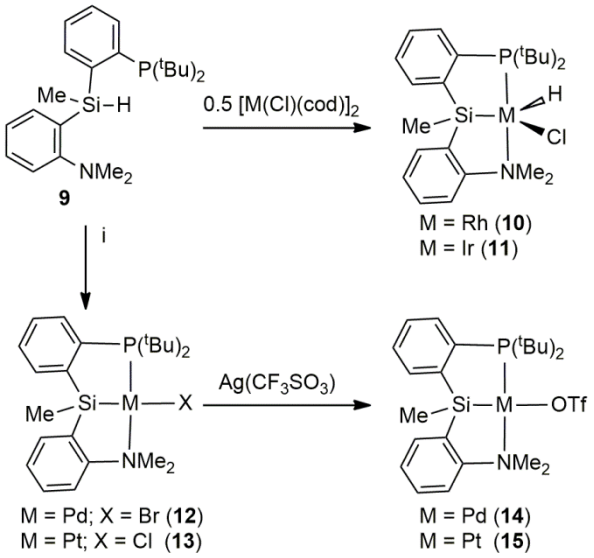

Scheme 4. Examples of transition metal complexes with monoanionic PSiN ligands, (i) M = Pd, $PdBr_2$ and NEt_3; M = Pt, $[PtCl_2(cod)]$ and NEt_3.

2.2. Reactivity of NSiN ligand precursors with group 8 metals.

The chemistry of group 8 transition metals with monoanionic NSiN ligands has been scarcely explored. Indeed, as far as we know the above mentioned Os-*fac*-κ^3-(*Si*,*N*,*N*)-NSiN complex **5** represents the only example reported so far [20]. In this context, it should be noted that the reaction of the NSiN ligand precursor **1** (Scheme 1) with $[Fe\{N(SiMe_3)_2\}_2]$ yields the iron complex $[Fe(\kappa^2$-*H*,*N*-**1**$)\{N(SiMe_3)_2\}_2]$ (**16**) containing an η^1-(Si-H)-Fe interaction (Scheme 5). The solid state structure of **16** has been confirmed by X-ray studies [25]. The Si-H bond distance (1.464(17) Å) is within the expected range. However, the Fe-H bond distance of 1.926(17) Å is rather long. Additionally, the Si atom is located at 3.06(2) Å from the Fe. This value is longer than the sum of their respective covalent radii (2.63 Å) [25]. These evidences are in agreement with a η^1-(Si-H)-Fe coordination mode similar to that found for the

iridium cationic species [Ir(H)(HSiEt$_3$)(POCOP)][B(C$_6$F$_5$)$_4$] (**17**) (POCOP = 2,6-[OP(*t*Bu)$_2$]$_2$C$_6$H$_3$) [26].

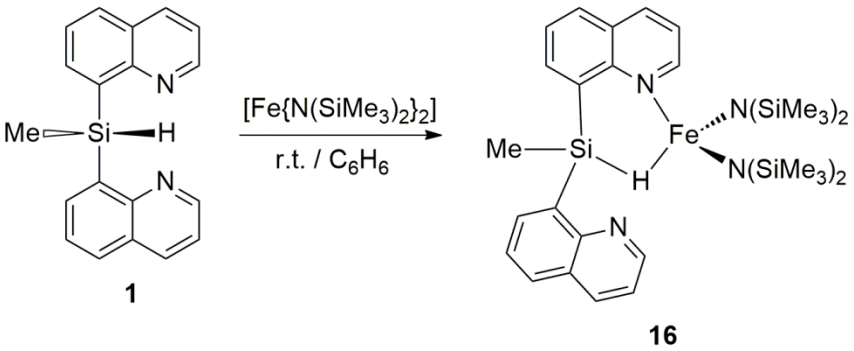

Scheme 5. Reactivity of compound **1** with [Fe{N(SiMe$_3$)$_2$}$_2$].

2.3. Reactivity of NSiN ligand precursors with group 9 metals.

2.3.1. Rh-NSiN complexes.

The reaction of the Wilkinson´s catalyst [Rh(Cl)(PPh$_3$)$_3$] with compound **1** in dichloromethane affords the rhodium(III) species [Rh(H)(Cl){*fac*-κ^3-(*Si*,*N*,*N*)-NSiN^A}(PPh$_3$)] (**18**), which was isolated as a yellow crystalline solid (Scheme 6) [17]. The formation of **18** entails substitution of two PPh$_3$ ligands by the nitrogen donor atoms in **1** as well as the oxidative addition of the Si-H bond to the rhodium(I) center to give the rhodium(III) silyl hydride species **18**. The ^{29}Si{^{1}H} NMR spectra of **18** show the resonance assigned to the silicon atom as a multiplet at δ 40.3 ppm, highly low field shifted with respect to the value of δ -18.9 ppm reported for **1** [17].

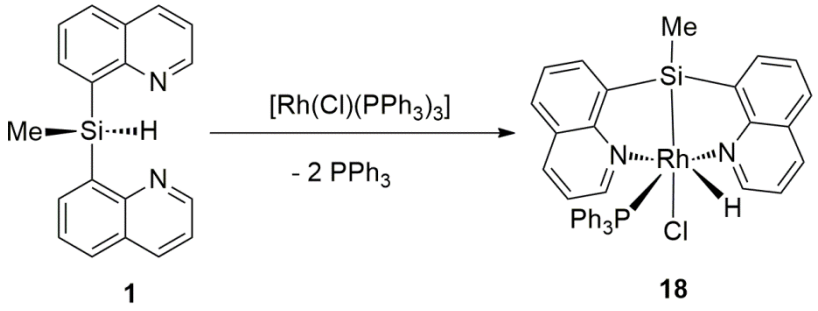

1 **18**

Scheme 6. Reaction of compound **1** with [Rh(Cl)(PPh_3)$_3$].

Reactivity studies showed that the rhodium(III) complex **18** reacts with DBU (1,8-Diazabicyclo[5.4.0]undec-7-ene), a strong non-nucleophilic Lewis base, in dichloromethane to give the dichlorinated species [Rh(Cl_2){*fac*-κ^3-(*Si*,*N*,*N*)-$NSiN^A$}(PPh_3)] (**19**) (Scheme 7). X-ray diffraction studies of **19** show that the Rh-Cl bond *trans* to the silicon atom is longer (2.640(2) Å) than the Rh-Cl bond *trans* to the nitrogen atom of the quinolyl group (2.356(2) Å) [17]. In addition, treatment of complex **18** with three equivalents of PMe_3 in CH_2Cl_2 leads to the highly symmetric bis-phosphine cationic species [Rh(Cl){*fac*-κ^3-(*Si*,*N*,*N*)-$NSiN^A$}(PMe_3)$_2$]Cl (**20**) (Scheme 7) [17]. Thus, the Rh-H bond in **18** could be deprotonated by strong Lewis bases in chlorinated solvents.

On the other hand, the reaction of complex **18** with 2.0 equiv of Mg(CH_2Ph)Cl produces abstraction of the hydride ligand instead of the chloride ligand to give the benzyl derivative **21** (Scheme 7) [17].

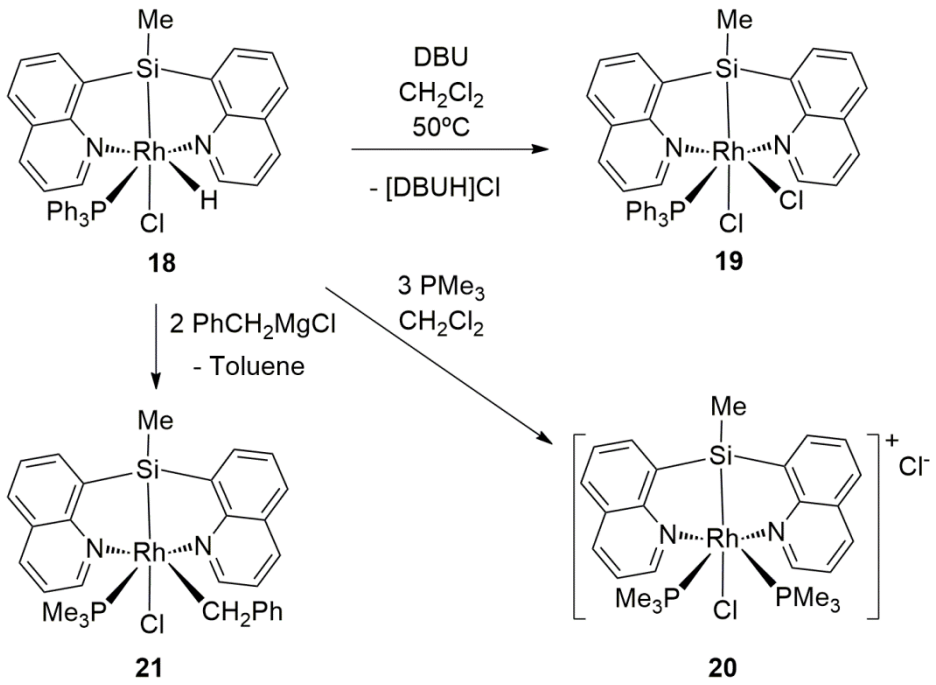

Scheme 7. Selected examples of the reactivity of compound **18**.

The rhodium(III) complex $[RhCl_3(NCMe)_3]$ has also proven to be useful as metallic precursor for the synthesis of Rh-NSiN^A species. Thus, its treatment with the ligand precursor **1** in CH_2Cl_2 and in presence of NEt_3 leads to the formation of the chloro-bridged binuclear complex $[Rh(Cl)_2\{fac\text{-}\kappa^3\text{-}(Si,N,N)\text{-}NSiN^A\}]_2$ (**22**) (Scheme 8) [17]. Among the examples of reactivity reported for complex **22** it is noteworthy to point out that its reaction with $Mg(CH_2Ph)Cl$, which affords the dibenzyl derivative $[Rh(CH_2Ph)_2\{fac\text{-}\kappa^3\text{-}(Si,N,N)\text{-}NSiN^A\}]$ (**23**). The solid state structure of **23** could be unambiguously determined by X-ray diffraction studies (Scheme 8) [17].

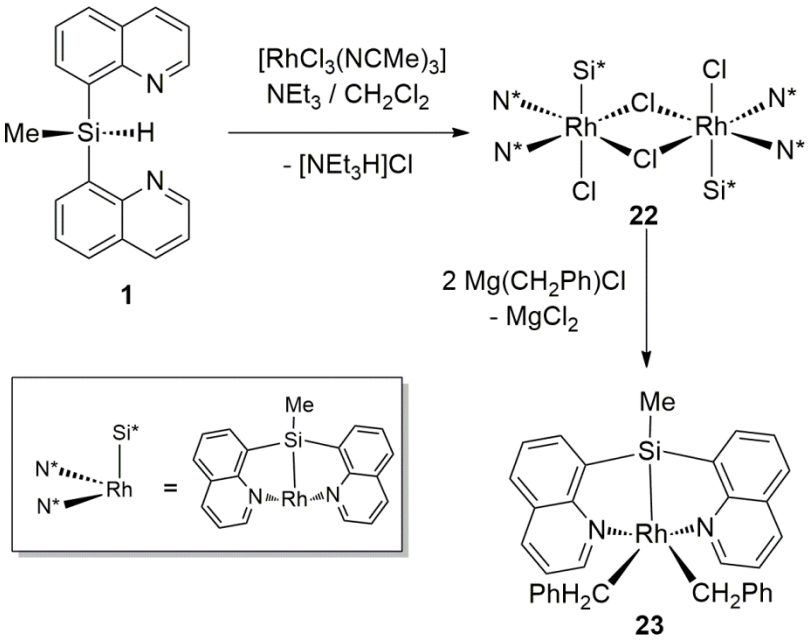

Scheme 8. Preparation and reactivity of the binuclear complex **22**.

The compound bis(pyridine-2-yloxy)methylsilane (**3**) (Scheme 1) has also been successfully employed as ligand precursor for the synthesis of Rh-NSiN complexes [18]. The reaction of compound **3** with the rhodium(I) species $[RhCl(coe)_2]_2$ in toluene affords the rhodium(III) complex [Rh(H)(Cl){*fac*-κ^3-(*Si*,*N*,*N*)-NSiN^C}(coe)] (**24**), which was found to be highly unstable and could not be isolated (Scheme 9). However, it should be mentioned that toluene solutions of in situ prepared complex **24** could be successfully employed as chemical reagent. Thus, the treatment of toluene solutions of **24** with the stoichiometric amount of AgOTf quantitatively yields the triflate derivative [Rh(H)(CF_3SO_3){*fac*-κ^3-(*Si*,*N*,*N*)-NSiN^C}(coe)] (**25**) (Scheme 9). In addition, in situ generated toluene solutions of **24** reacts with PCy_3 to afford the rhodium-phosphane complex [Rh(H)(CF_3SO_3){*fac*-κ^3-(*Si*,*N*,*N*)-NSiN^C}(PCy_3)] (**26**) (Scheme 9) [18]. The solid state structures of complexes **25** and **26** were determined by X-ray diffraction studies. It should be noted that the Rh-Cl

bond distance in **26** (2.**51**69(6) Å) is shorter than that found for the Rh-Cl bond *trans* to the silicon atom in the related complex **19** (2.640(2) Å). This is in agreement with a weaker *trans* influence of the silyl group in **26** in comparison with **19**.

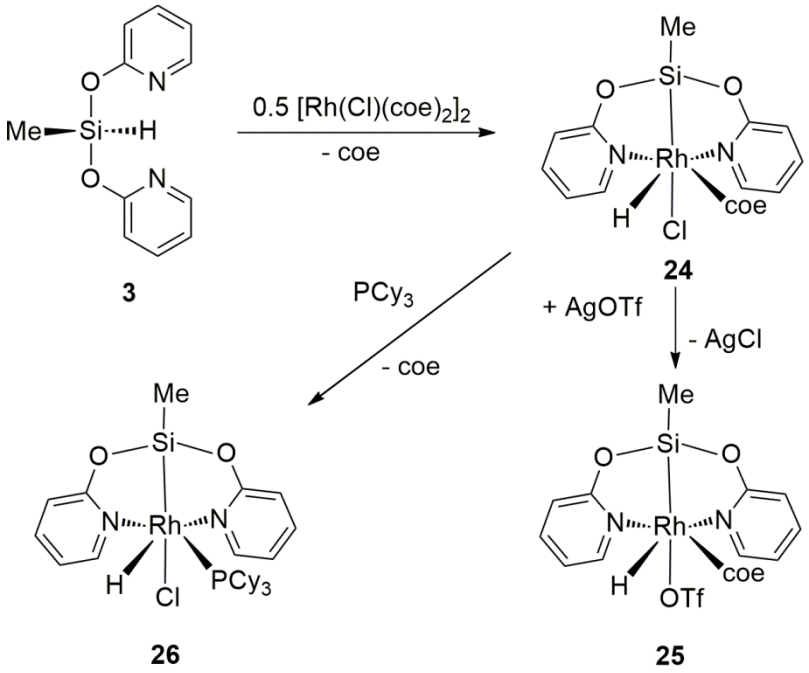

Scheme 9. Preparation and reactivity of Rh-NSiN^{C} complexes.

2.3.2. Ir-NSiN complexes.

The chemistry of Ir-NSiN compounds is more developed than that of the analogous Rh-NSiN species. This could be attributable to a higher stability of Ir-NSiN complexes compared with the related rhodium derivatives. The iridium(I) binuclear complex $[IrCl_2(coe)_2]_2$ has proven to be an excellent metallic precursor for the synthesis of Ir-NSiN complexes. Thus, the reaction of $[IrCl_2(coe)_2]_2$ with the corresponding ligand precursor **1**, **3** or **4** quantitatively affords the respective iridium(III) species [Ir(H)(Cl){*fac*-κ^3-(*Si*,*N*,*N*)-NSiN}(coe)] (NSiN = NSiN^{A} (**27**) [15]; NSiN^{C} (**28**) [16a]; NSiN^{D} (**29**) [16b]) (Scheme 10). It should be mentioned that

while the related rhodium species **24** could not be isolated, these Ir-NSiN complexes have been isolated as yellow (**27**) and offwhite (**28**, **29**) solids. The $^{29}Si\{^{1}H\}$ NMR spectra of such compounds show the resonance corresponding to the silicon atom at δ -4.8 (**27**) [15], 31.5 (**28**) [16a] and 31.0 ppm (**29**) [16b]. Therefore, it could be concluded that the silicon atom in complexes **28** and **29** is electron poorer than that of **27**.

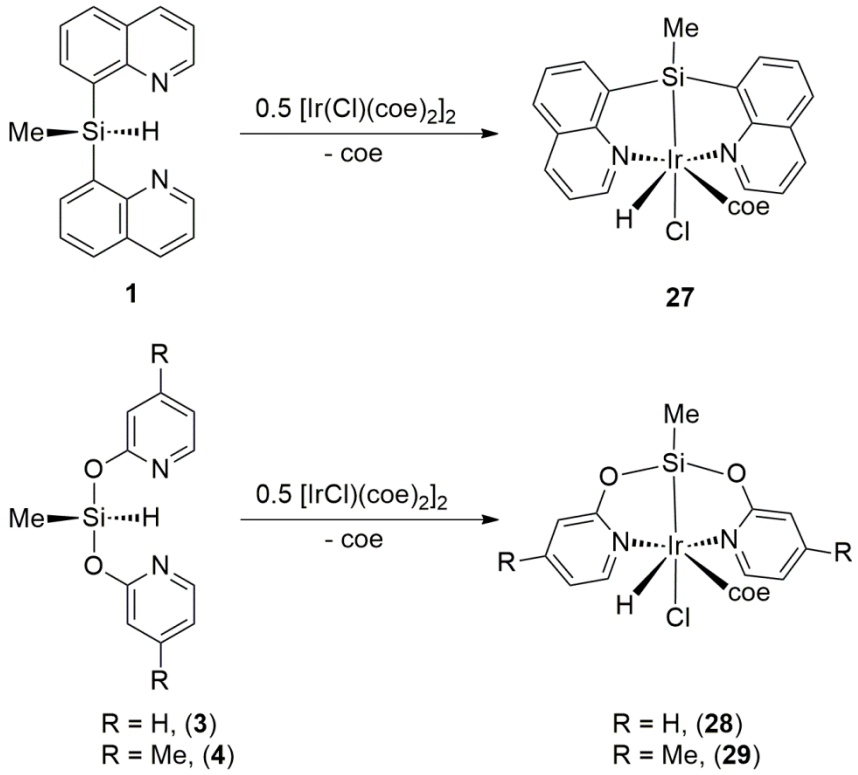

Scheme 10. Preparation of Ir-NSiN compounds.

The iridium compounds **27**-**29** behave similarly in their reactions with AgOTf in CH_2Cl_2. Thus, the corresponding triflate derivatives [Ir(H)(CF_3SO_3){*fac*-κ^3-(*Si*,*N*,*N*)-NSiN}(coe)] (NSiN = $NSiN^A$ (**30**) [15]; $NSiN^C$ (**31**) [16a]; $NSiN^D$ (**32**) [16b]) could be easily prepared in high yield by reaction of the respective chloride precursor with AgOTf. Interestingly, the Ir-$NSiN^A$ species **30** has shown a different chemical

behavior to the Ir-NSiN^{C} derivative **31** in its reactivity towards hydrosilanes in acetonitrile (Scheme 11). For instance; while the reaction of **30** with $HSiEt_3$ in acetonitrile affords cyclooctane and the ionic species [Ir($SiEt_3$){*fac*-κ^3-(*Si*,*N*,*N*)-NSiN^{A}}$(NCMe)_2$][TfO] (**33**) with two coordinate acetonitrile molecules [15], under the same reaction conditions complex **31** is transformed into the neutral compound [Ir($SiEt_3$)(CF_3SO_3){*fac*-κ^3-(*Si*,*N*,*N*)-NSiN^{C}}(NCMe)] (**34**) [27]. The reason behind this different behavior could be a lower *trans* influence of silyl group in **31** than in **30**. Indeed, the $^{29}Si\{^{1}H\}$ NMR spectra of **30** show the resonance corresponding to the silicon atom at δ -8.2 ppm [15] high field shifted in comparison with that observed for **31** (δ 13.6 ppm) [16a].

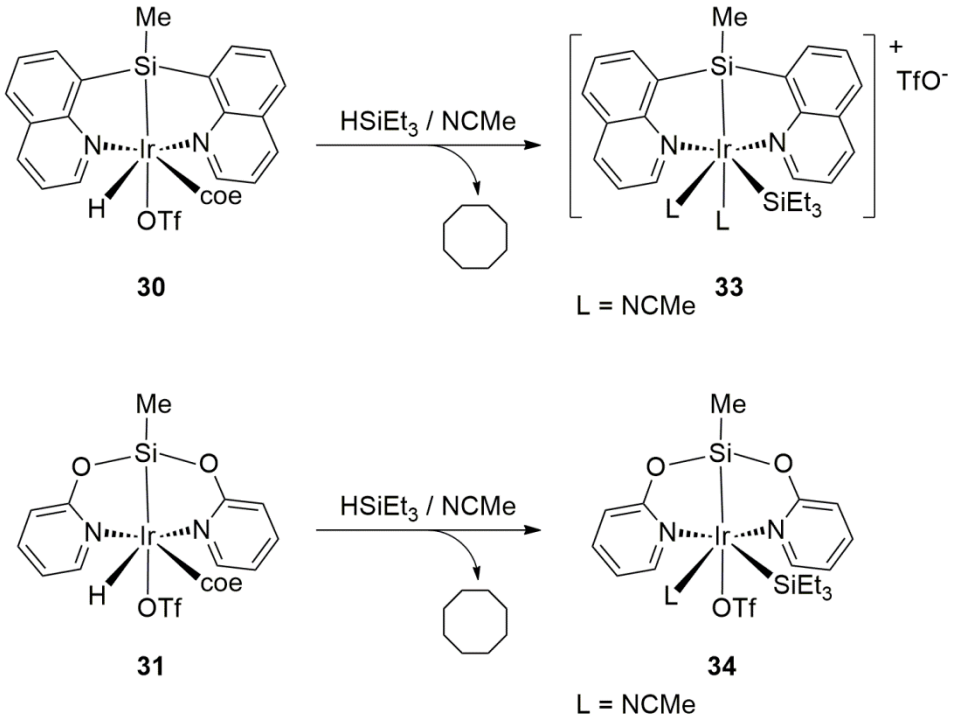

Scheme 11. Reactivity of acetonitrile solutions of complexes **30** and **31** with $HSiEt_3$.

The addition of one equivalent of PR_3 (R = Ph, Me) to CH_2Cl_2 solutions of complex **27** promotes the substitution of the coe ligand by the phosphine to give the corresponding species [Ir(H)(Cl){*fac*-κ^3-(*Si*,*N*,*N*)-$NSiN^A$}(PR_3)] (R = Ph, **35**; Me, **36**) (Scheme 12). Interestingly, if a large excess of PMe_3 (10 equiv) is added to the reaction medium, not only the dissociation of the chloride ligand *trans* to the silyl group but also decoordination of one of the N-heterocyclic rings of the NSiN ligand is favored. Thus, under these reaction conditions the species [Ir(H){κ^2-(*Si*,*N*)-$NSiN^A$}(PMe_3)$_3$]Cl (**37**) containing the monoanionic $NSiN^A$ ligand in bidentate κ^2-*Si*,*N* coordination mode is formed (Scheme 12) [15].

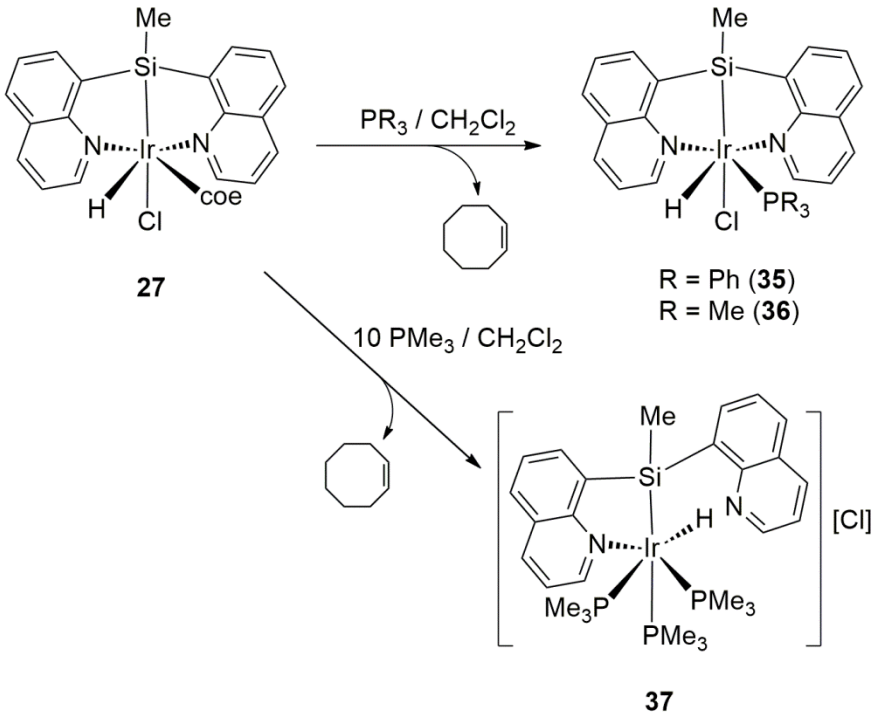

Scheme 12. Reactivity of complex **27** with phosphines.

In this context, it should be noted that the reaction of compound **1** with [Ir(CH_3)(PMe_3)$_4$] affords the complex [Ir(H)(CH_3){κ^1-(*Si*)-$NSiN^A$}(PMe_3)$_3$] (**38**)

with the corresponding $NSiN^A$ ligand in a κ^1-*Si*-monodentate coordination mode (Scheme 13) [15].

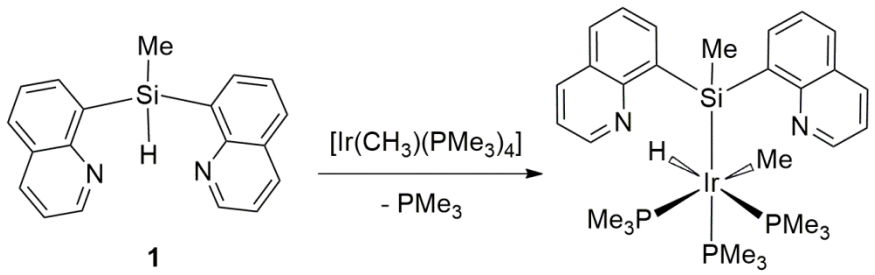

Scheme 13. Reaction of compound **1** with $[Ir(CH_3)(PMe_3)_4]$.

Thus, most of the reported Ir-NSiN species contain the monoanionic NSiN ligand in κ^3-*Si*,*N*,*N*-tridentate coordination mode. However, examples of Ir-$NSiN^A$ complexes containing such ligand in κ^2-*Si*,*N*-bidentante- and κ^1-*Si*-monodentate coordination modes are also known [15]. In addition, it may be worth mentioning that a relation between the hapticity of the NSiN ligand and the chemical shift of the silicon atom in the $^{29}Si\{^1H\}$ NMR spectra of such complexes has been found. Thus, the mentioned resonance appears centered at δ 0.85, -6.0 or -9.4 ppm for complexes **36**, **37**, and **38**, respectively [15].

2.4. Reactivity of NSiN ligand precursors with group 10 metals.

2.4.1. Ni-NSiN complexes.

The nickel(0) $[Ni(cod)_2]$ species reacts with compound **2** in chlorobenzene to give the metallic cluster $[\{(NiCl)_2Ni\}(NSiN^B)_2]$ (**39**), which contains a $[Ni_3Si_2]$ core with two six-coordinate silicon atoms (Scheme 14) [21]. The X-ray and computational studies on **39** suggest that the $NSiN^B$ ligands play a central role in stabilizing the Ni_3

triangle. Moreover, complex **39** slowly evolves in CH_2Cl_2 to afford the mononuclear paramagnetic species (**40**) where the Si-phenyl moiety was coordinated to Ni in η^2-fashion (Scheme 14) [21].

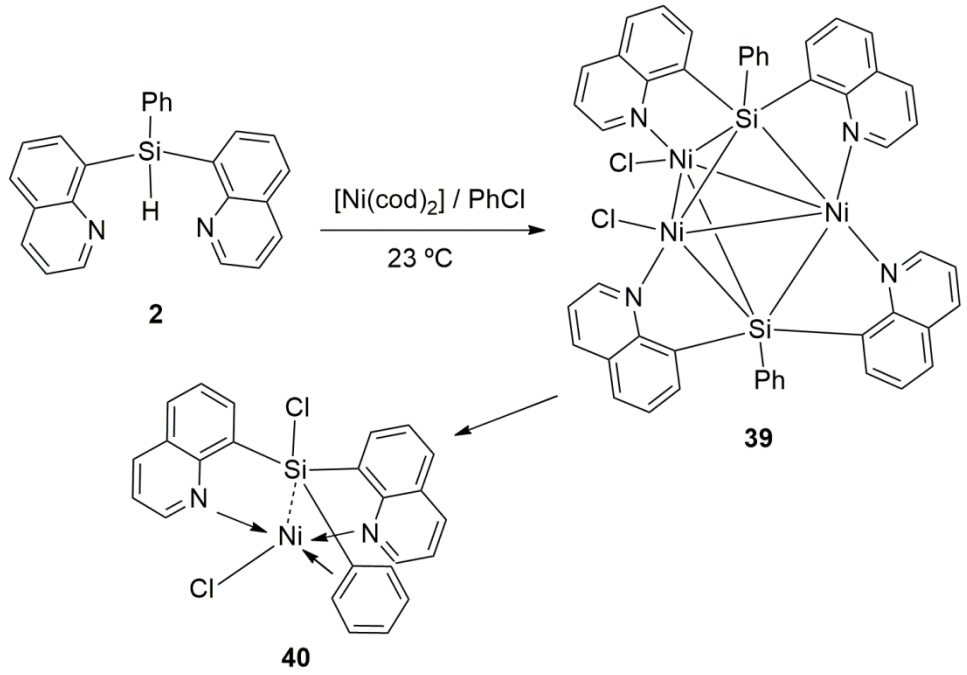

Scheme 14. Reactivity of compound **2** with $[Ni(cod)_2]$ and evolution of the resulting species **39**.

2.4.2. Pt-NSiN complexes.

In the case of platinum, different metal precursors have been successfully employed to prepare Pt-NSiN complexes. Thus, the Pt(II) species $[PtCl_2(cod)]$ reacts with one equivalent of the ligand precursor **1** in presence of NEt_3 to afford the square-planar Pt(II) complex $[Pt(Cl)\{\kappa^3\text{-}(Si,N,N)\text{-}NSiN^A\}]$ (**41**) (Scheme 15) [19a]. It was also observed that the reaction of $[PtCl_2(cod)]$ with two equivalents of **1** in absence of an additional bases yields, after heating at 60 ºC for 36 h, a mixture of the Pt(IV) species $[Pt(H)_2(Cl)\{fac\text{-}\kappa^3\text{-}(Si,N,N)\text{-}NSiN^A\}]$ (**42**) and bis-(8-quinolyl)methylchlorosilane

(**43**) (Scheme 15) [19a]. The Pt(II) complex [Pt(Me)$_2$(tmeda)] behaves differently to [PtCl$_2$(cod)]. Thus, when [Pt(Me)$_2$(tmeda)] solutions in benzene were heated at 80ºC in presence of two equivalents of the NSiN ligand precursor **1** the formation of the platinum(II) species [Pt{*cis*-(κ^2-(*Si*,*N*)-NSiN^A)$_2$}] (**44**) and methane was observed (Scheme 15). The *cis* disposition of the κ^2-(*Si*,*N*)-NSiN^A ligands in **44** was additionally supported by comparison with the related Pd(II) complex [Pd{*cis*-(κ^2-(*Si*,*N*)-NSiN^A)$_2$}] (**45**) [19a] where the X-ray crystal structure reveals a distorted squareplanar geometry with two *cis* NSiN^A ligands binding to the metal thought one nitrogen and the corresponding silyl group [19a].

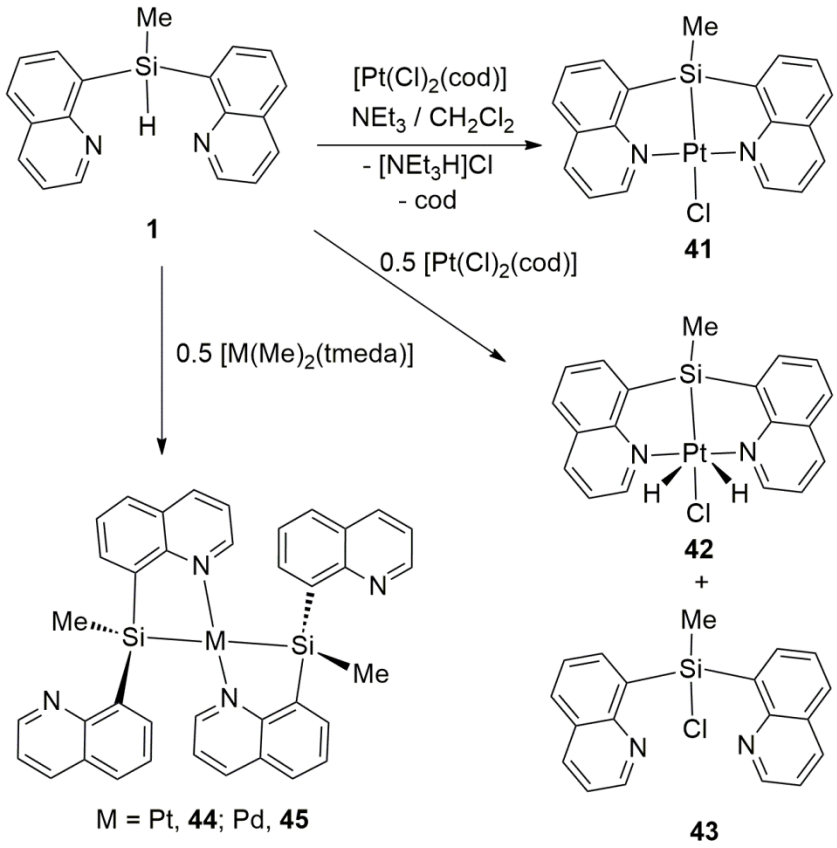

Scheme 15. Reactivity of Pt(II) and Pd(II) precursors with compound **1**.

On the other hand, the Pt(IV) tetramers $[PtMe_3X]_4$ (X = I; CF_3SO_3) react with compound **1** to give the corresponding Pt(IV) species $[Pt(Me)_2(I)\{fac\text{-}\kappa^3\text{-}(Si,N,N)\text{-}NSiN^A\}]$ (X = I, **46**; CF_3SO_3, **47**) (Scheme 16) [19a]. In this regard, it should be noted that the related Pt(IV) species $[Pt(COMe)_2(Cl)\{fac\text{-}\kappa^3\text{-}(Si,N,N)\text{-}NSiN^A\}]$ (**48**) was obtained by reaction of the ligand precursor **1** with half equiv of $[Pt_2\{(COMe)_2H\}_2(\mu\text{-}Cl)]$ [19b].

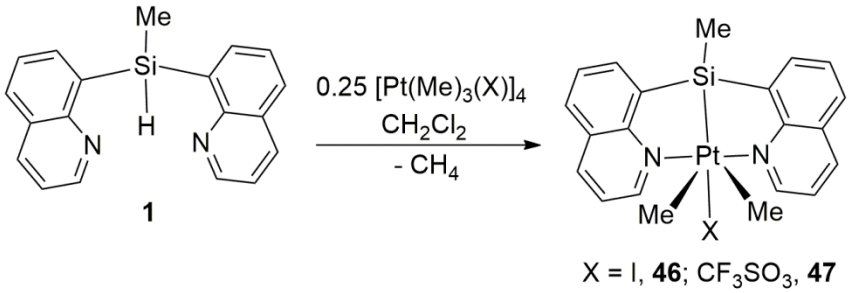

Scheme 16. Reactivity of $[Pt(Me_3)X]$ (X = I, CF_3SO_3) with compound **1**.

In this context, it should be mentioned that the reaction of the Pt(II) complex $[PtMe_2(bps)]$ (**48**) (bps = bis(2-pyridyl)dimethylsilane) with H_2O_2 or O_2/MeOH leads to the Pt(IV) species $[PtMe_3(fac\text{-}\{\kappa^3\text{-}N,N,O\text{-}(2\text{-}C_5H_4N)_2SiMeO\})]$ (**49**) [28].

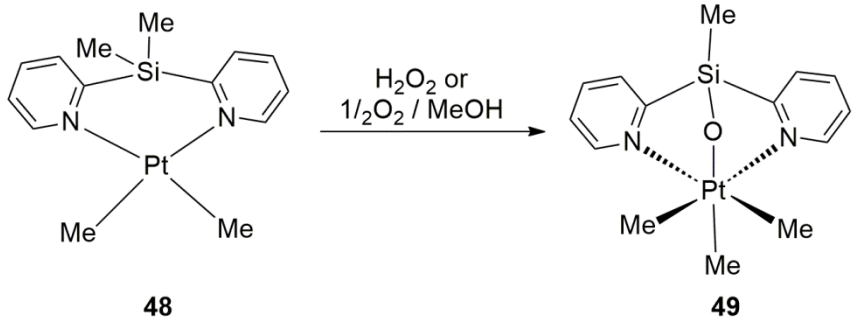

Scheme 17. Reactivity of $[PtMe_2(bps)]$ (**48**) (bps = bis(2-pyridyl)dimethylsilane) with H_2O_2 or O_2/MeOH.

3 Homogeneous catalytic processes based on metal-NSiN complexes.

3.1. Rh-NSiN catalyzed processes

The transition metal-catalyzed reaction of ketones with hydrosilanes commonly undergoes hydrosilylation of the carbonyl group [29, 30]. In addition, examples of main group-catalyzed hydrosilylation and hydroboration of carbonyl compounds to the corresponding silyl or boryl-ether are also known [31]. Nevertheless, some examples of catalytic dehydrogenative silylation of ketones to give silyl enol ethers have also been reported [29, 32, 33, 34]. Silyl enol ethers are chemicals of significant interest due to their application as reagents in organic chemistry [35]. Recently, the rhodium(III) complex [Rh(H)(CF_3SO_3){*fac*-κ^3-(*Si*,*N*,*N*)-$NSiN^C$}(coe)] (**25**) (Scheme 9) has been successfully employed as catalyst precursor for the synthesis of silyl enol ethers from the reaction of acetophenone derivatives with hydrosilanes (Scheme 18) [18].

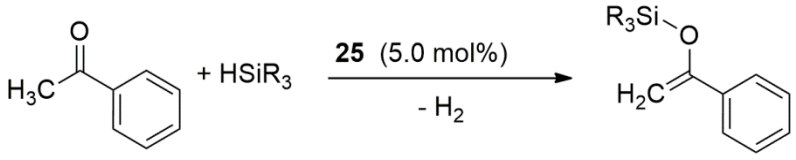

Scheme 18. **25**-catalyzed dehydrogenative silylation of ketones to give silyl enol ethers.

A mechanism based on experimental and computational studies has been proposed for such reaction (Scheme 19). The overall process could be summarised in four steps, which includes: i) Reaction of complex **25** with one equivalent of silane to release cyclooctane and afford the active catalytic species **A**, ii) ligand assisted heterolytic cleavage of the Si-H bond of the silane to affords **B**, iii) the dehydrogenative silylation of the activated acetophenone throught intermediate **C** to

give the respective silyl enol ether **D**, molecular hydrogen and intermediate **A**, and iv) the catalytic cycle for hydrogenation of **D** via intermediates **E** and **F** to give the corresponding silyl ether **G** and the active species **A**. The highest energy barrier of the overall process (20.9 kcal mol^{-1}) corresponds to the activation of the Si-H bond. The formation of the silyl ether **G** towards the silyl enol ether **D** is thermodynamically favored by 4.3 kcal mol^{-1}. However, in an open system the irreversible released of molecular hydrogen from intermediate **C** yields the silyl enol ether **D** to regenerate the active species **A** and therefore, inhibits the side catalytic cycle which leads to the silyl ether **G**. This is in accordance with the experimental findings, which evidenced that the silyl enol ether species **D** is the major reaction product under these reaction conditions (Scheme 19) [18].

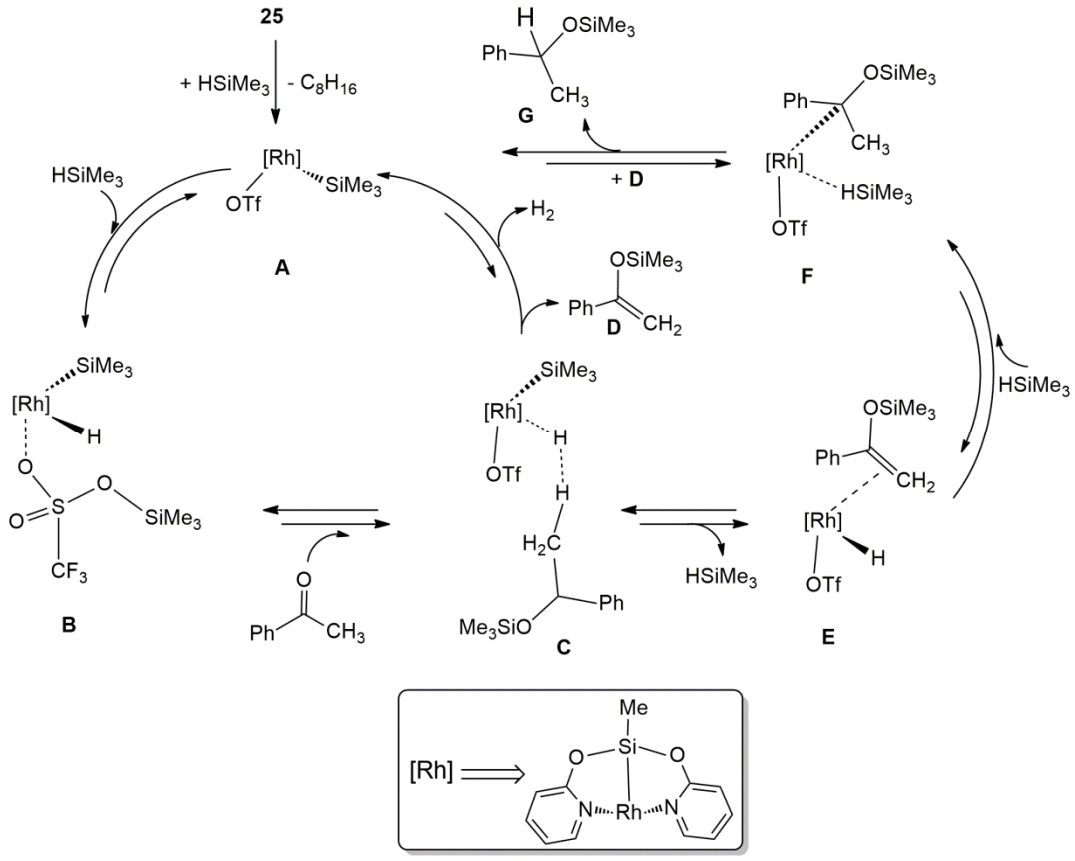

Scheme 19. Mechanism proposed for the **25**-catalyzed dehydrogenative silylation of ketones to give silyl enol ethers [18].

3.2. Ir-NSiN catalyzed processes

3.2.1. Catalytic dehydrogenative silylation of arenes

The catalytic dehydrogenative silylation of unactivated C−H bonds is a target of great importance due to the application of silyl arenes and vinyl silanes as reagents for organic synthesis and materials science [36]. The iridium complex [Ir(H)(CF_3SO_3){*fac*-κ^3-(*Si*,*N*,*N*)-$NSiN^A$}(coe)] (**30**) catalyzes the reaction of $HSiPh_3$ with C_6D_6 at 120 ºC in presence of norbornene as hydrogen acceptor to quantitatively yield the corresponding silyl derivative $C_6D_5(SiPh_3)$ after 24h (Scheme 20) [15b]. Under the same reaction conditions monosubstituted arenes C_6H_5X (X = CF_3, Cl, CH_3) were silylated to give mixtures of *m*- and *p*-silylated species. The electron-withdrawing character of the arene substituent influences the reaction rate. Thus, the following reactivity trend has been reported for C_6H_5X species (X = CF_3 > Cl > CH_3 > H) [15b].

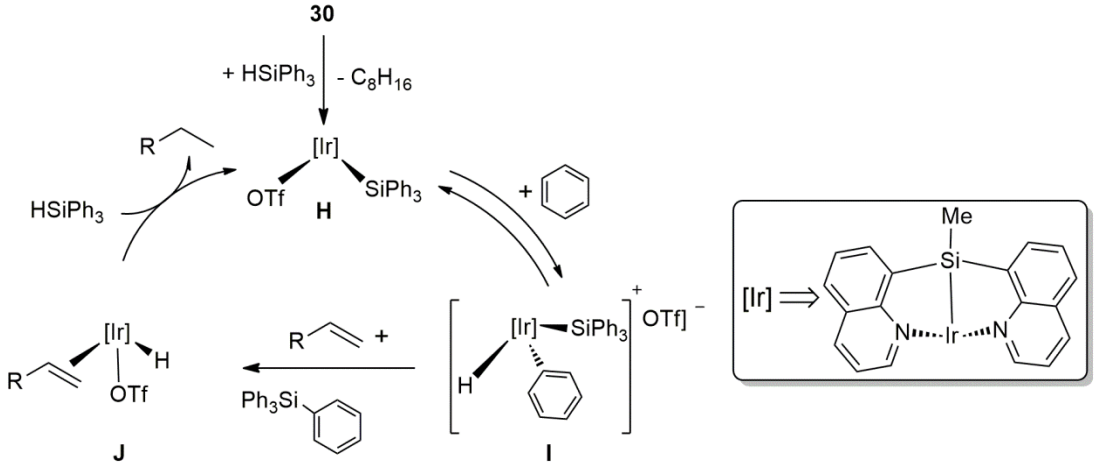

Scheme 20. Mechanism proposed for the **30**-catalyzed (10 mol%) dehydrogenative silylation of arenes [15b].

Scheme 20 summarizes the mechanism proposed for the **30**-catalyzed dehydrogenative silylation of arenes. This mechanism implies the oxidative addition of one C-H bond of the arene to the active species **H** to afford the Ir(V) intermediate **I**, which reductively eliminates $C_6H_5(SiPh_3)$ and coordinates one molecule of alkene to give the reaction intermediate **J**. The last step of the process embraces the migratory insertion of the olefin into the Ir-H bond of **J**, followed by reaction with one equivalent of $HSiPh_3$ to afford the active species **H** and the corresponding alkane (Scheme 20) [15b]. In this regard, it should be mentioned that although iridium(V)-NSiN species have not been isolated so far, examples of iridium(V) silyl derivatives containing isoelectronic ligands such as η^5-cyclopentadienyl [37] or κ^3-trispyrazolylborate ligands [38] are known.

3.2.2. Catalytic hydrosilylation of CO_2

The catalytic reaction of CO_2 with hydrosilanes constitutes an example of thermodynamically favored CO_2-reduction process which has been extensively studied during the last few years [39]. Particularly, Ir-NSiN complexes have proven to be highly active and selective catalysts for the solvent-free hydrosilylation of CO_2 to give the corresponding silyl-formate [16]. A summary of the mechanism proposed for the **31**-catalyzed reaction of CO_2 with hydrosilanes is shown in Scheme 21 [16a]. The overall catalytic cycle could be understood as a three steps process involving; i) catalyst activation and η^2-Si-H coordination of one molecule of silane to give intermediate **K**, ii) triflate assisted Si-H bond activation via **TSKL** transition state to give **L** and iii) formation of the κ-*O*-coordinated silylformate molecule via **TSLM** transition state to afford intermediate **M** from which the molecule of silyl formate is

released to regenerate the active species **K**. The higher energetic barrier of the catalytic process (18.9 kcal mol^{-1}) corresponds to the Si-H bond activation step which corresponds to the concerted transition state **TSKL** (Scheme 21) [16a].

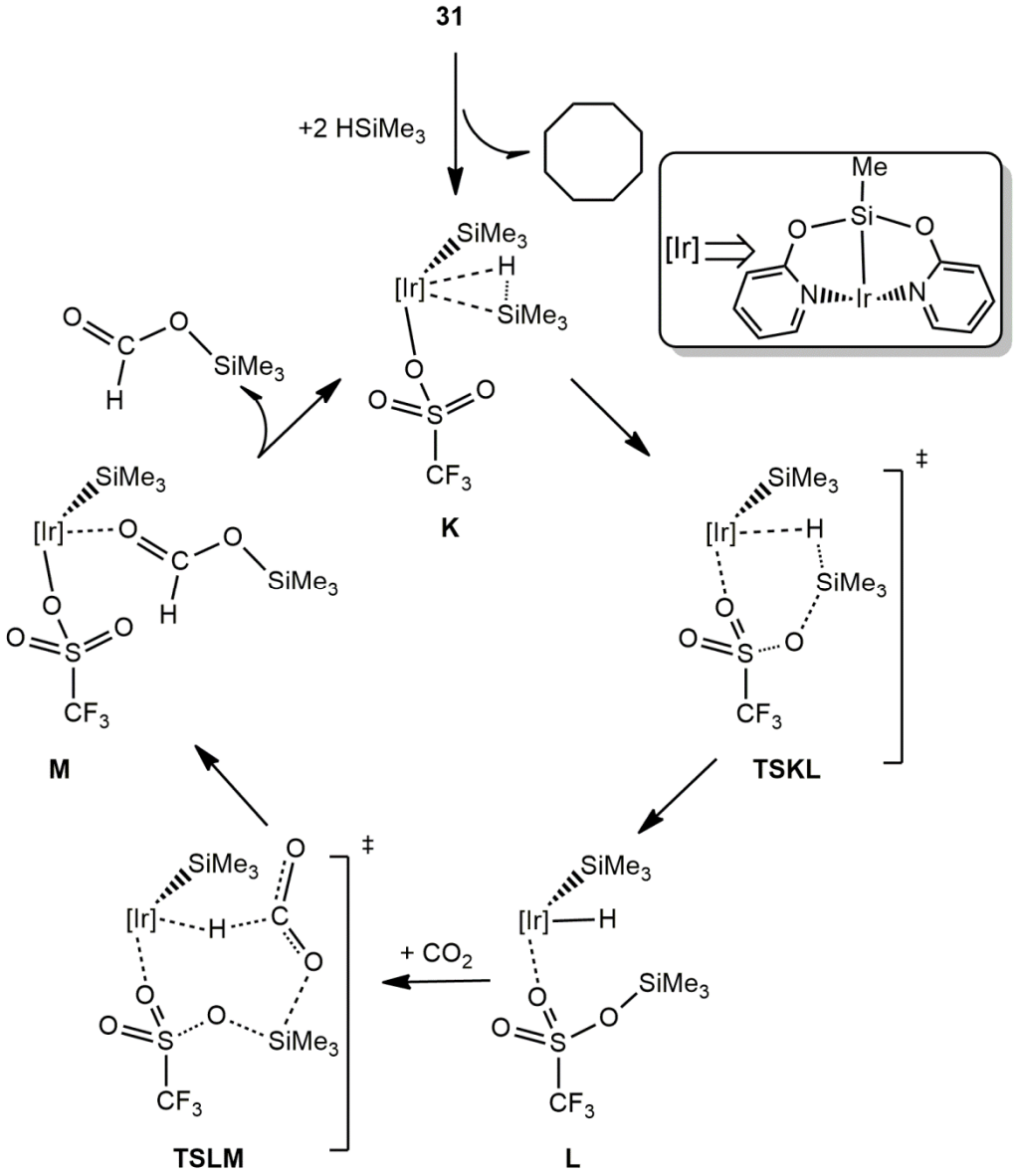

Scheme 21. Proposed mechanism proposed for the solvent-free **31**-catalyzed (1.0 mol%) hydrosilylation of CO_2.

Accordingly with the **TSLM** transition state it is reasonable to propose that the nucleophilic attack of the hydride to the carbon atom of the CO_2 molecule could determinate the rate of the CO_2 activation process (Scheme 21). Thus, it would be expected that an enhancement of the electron-donor ability of the ancillary ligands and of the N-heterocyclic rings of the NSiN ligand would increase the electronic density around the hydride and therefore the catalytic activity of the resulting catalyst. Indeed, the catalytic precursor [Ir(H)(CF_3CO_2){*fac*-κ^3-(*Si,N,N*)-$NSiN^D$}(coe)] (**50**), containing a trifluoroacetate ancillary ligand and a 4-methyl substituent at the N-heterocyclic rings showed the highest catalytic activity and selectivity as CO_2-hydrosilylation catalyst among the series of Ir-NSiN complexes studied so far [16, 40].

3.2.3. Catalytic reactions of CO_2 with secondary amines and hydrosilanes

The catalytic reaction of CO_2 with hydrosilanes and secondary (or primary) amines commonly leads to the formation of the respective formamide or methyl amine depending on the reaction conditions [41]. However, the solvent-free reactions of CO_2 with $HSiMe(OSiMe_3)_2$ and secondary amines (pyrrolidine, Et_2NH, *i*Pr_2NH or BnMeNH) leads to the corresponding silyl carbamate as major reaction product in around 90 % yield [42]. The explanation for this different behavior was found to be that under these reaction conditions, the active species **K** (Scheme 21) promotes the dehydrogenative silylation of the corresponding secondary amine to give the respective silyl amine. This reaction is faster than the above described CO_2 hydrosilylation. Subsequently, the insertion of CO_2 into the Si-N bond of the in-situ generated silyl amine affords the corresponding silyl carbamate (Scheme 22) [42].

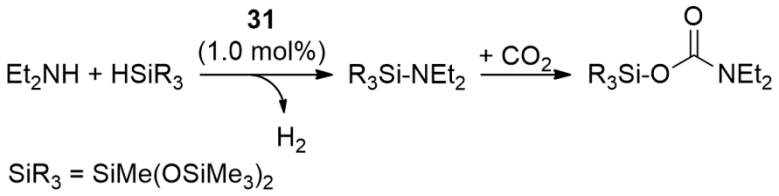

Scheme 22. Solvent-free **31**-catalyzed reaction of CO_2 with $HSiMe(OSiMe_3)_2$ and Et_2NH.

The above described catalytic dehydrogenative silylation and subsequent CO_2-insertion in the resulting Si-N bond allows explanation for the selective formation of silyl carbamates from aliphatic amines (Scheme 22). Conversely, when aromatic secondary amines were used under the same reaction conditions, a drastic decrease of the selectivity and activity was observed. Theoretical calculations showed that the determining step of the process is the Si-H bond activation to give intermediate **N**, which was found to be assisted by interaction of the lone electron pair of the amine with the silicon atom via **TSKN** (Scheme 23). Therefore, the weaker Lewis base character of aromatic secondary amines compared to that of aliphatic amines could explain the observed reactivity trend [42]. Intermediate **N** evolves to give **O**, which reacts with one equivalent of silane to afford the corresponding silyl amine, molecular hydrogen and the active species **K** (Scheme 23).

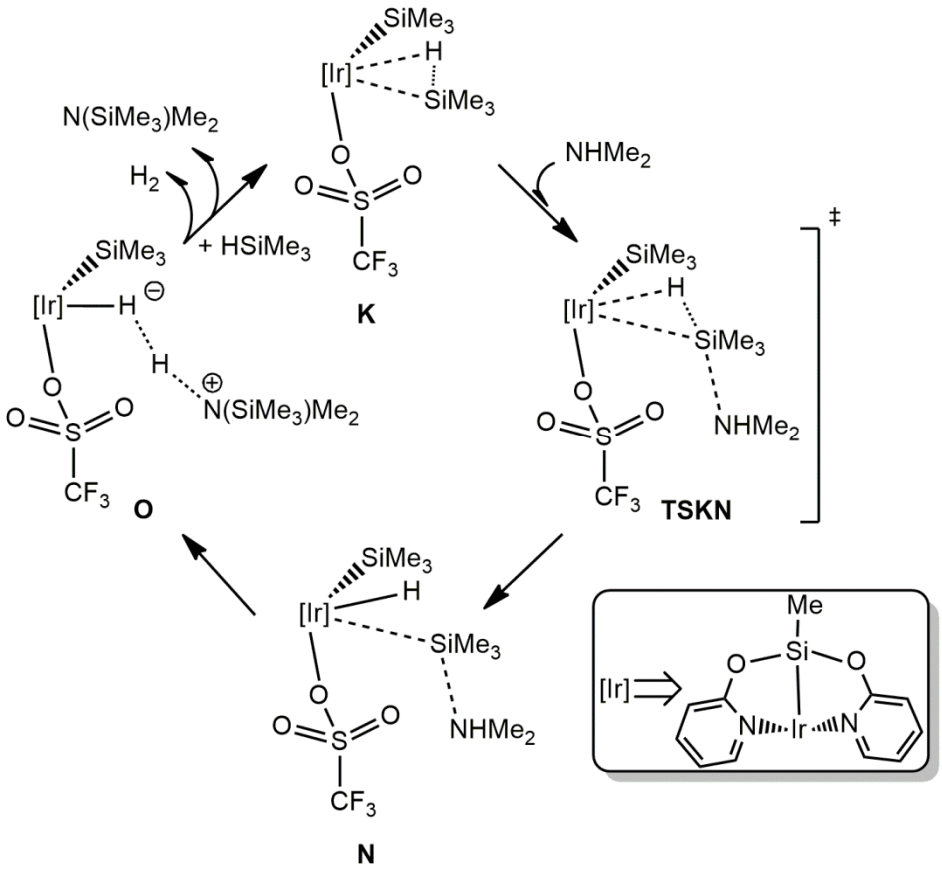

Scheme 23. Proposed mechanism for the **31**-catalyzed synthesis of silyl carbamates from reaction of CO_2 with silanes and amines.

3.2.4. Catalytic reactions of CO_2 with silyl phosphines

The insertion of CO_2 into the P-Si bond of silyl phosphines has been scarcely studied. The main reason could be the high reactivity of the resulting silylphosphinecarboxylate, which easily evolves in protic medium to yield CO_2, siloxanes and the corresponding secondary phosphine [43]. In this regards, it should be mentioned that some examples of silylphosphinocarboxylates stabilized by coordination to the boron atom of $B(p\text{-}C_6F_4H)_3$ [44] or to Cr(0) or W(0) pentacarbonyl fragments are known [45].

Interestingly, the Ir-NSiN^C complex **31** catalyzes the reaction of $P(SiMe_3)Ph_2$ with CO_2 to quantitatively give the corresponding insertion product $P(CO_2SiMe_3)Ph_2$ (**51**)

which could be characterized by NMR spectroscopy (Scheme 24) [46]. Complex **31** has shown much more activity than **28**. Thus, while using complex **28** as catalyst precursor 24 h were needed to achieved the full conversion of $P(SiMe_3)Ph_3$ into **51**, with **31** the reaction was completed after 20 min. It should be noted that the stepwise reactions of **28** with $P(SiMe_3)Ph_2$ and with CO_2 according to Scheme 24 were monitored by ^{1}H, $^{13}C\{^{1}H\}$ and $^{31}P\{^{1}H\}$ NMR spectroscopies. These NMR studies allowed to characterize the reaction intermediates [Ir(H)(Cl){*fac*-κ^3-(*Si,N,N*)-$NSiN^C$}{$P(SiMe_3)Ph_2$}] (**52**) and [Ir(H)(Cl){*fac*-κ^3-(*Si,N,N*)-$NSiN^C$}{$P(CO_2SiMe_3)Ph_2$}] (**53**) (Scheme 24) [46]. Moreover, it has been proven that the reaction of the in situ prepared complex **53** with one equivalent of $P(SiMe_3)Ph_3$ releases the phosphinecarboxylate species **51** to afford complex **52** (Scheme 24).

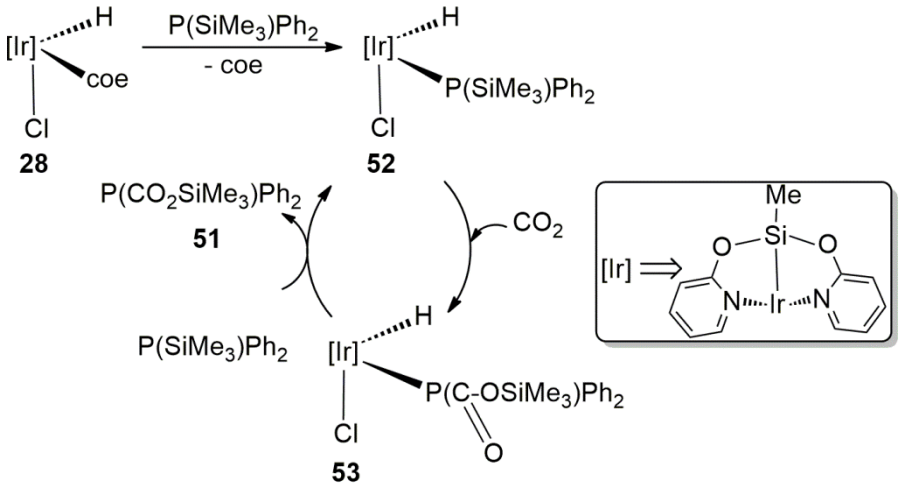

Scheme 24. Reaction of CO_2 (4 bar) with $P(SiMe_3)Ph_2$ in presence of catalytic amounts of complex **28**.

Theoretical calculations showed that the overall process is exergonic, thermodynamically favored by 13.5 kcal mol^{-1} and that the highest energetic barrier of the processes (25.4 kcal mol^{-1}) corresponds to the P-Si bond activation step [46].

3.2.5. Catalytic generation of hydrogen from water and hydrosilanes

The reaction of the Si-H bond of hydrosilanes with water to afford H_2 and the corresponding silanol is a thermodynamically favourable process. Some examples of homogeneous [47] and heterogeneous [48] catalytic systems for the hydrolysis of hydrosilanes have been already reported. The iridium(III) complex [Ir(H)(CF_3SO_3){*fac*-κ^3-(*Si*,*N*,*N*)-$NSiN^C$}(coe)] (**31**) has shown to be a highly active catalyts precursor for hydrogen generation by hydrolysis of hydrosilanes [27]. It was observed that the catalytic activity of **31** depends both on the nature of the hydrosilane and the solvent. Indeed, high $TOF_{1/2}$ values were obtained from the hydrolysis of H_2SiEt_2 (107.140 h^{-1}), $(HSiMe_2)_2O$ (96.770 h^{-1}) or $HSiMePh_2$ (50.400 h^{-1}) in THF at 298 K [27]. Interestingly, although they are slower than those carried out in THF solution, the solvent-free reactions of $HSiMe(Me_3SiO)_2$ or $(HMe_2Si)_2O$ also produce hydrogen [27].

A reaction mechanism for this iridium-catalyzed process has been proposed based on experimental and computational studies (Scheme 25). The catalytic cycle could be schematically summarised as a two stages process involving; a) water assisted activation of the Si-H bond through the interaction of the oxygen atom of the water molecule with silicon atom of intermediate **P** to yield the zwitterionic intermediate **Q** and b) the water splitting process via a proton transfer from the cationic $[(H_2O)SiMe_3]^+$ moiety of **Q** to give intermediate **S**. This process could take place through two different pathways: water-assisted according to the Grotthuss

mechanism, path (i) or through intermediate **R**, path (ii). Path (i) is barrier-less and a low barrier (2.9 kcal mol^{-1}) has been found for path (ii) (Scheme 25). Once more, the highest energetic barrier of the overall process, 16.4 kcal mol^{-1}, corresponds to the Si-H bond activation step [27].

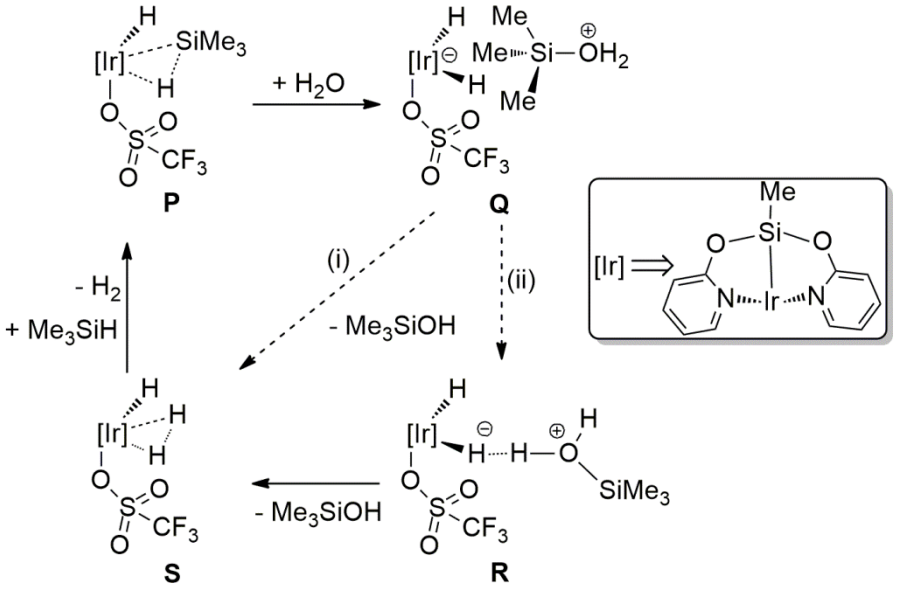

Scheme 25. Mechanism proposal for the **31**-catalyzed hydrolysis of silanes.

4 Conclusions.

This review illustrates that monoanionic NSiN ligands frequently coordinate to late transition metal complexes in a *fac*-κ^3-(*Si*,*N*,*N*)-tridentate coordination mode with pseudooctahedral geometry, although examples of square-planar Pt(II) κ^3-(*Si*,*N*,*N*)-NSiN complexes are also known. It is apparent that transition metal hydride complexes could be easily generated through the oxidative addition of the Si-H bond present in the corresponding NSiN ligand precursor to low valent transition metal species.

The chemistry of transition metal complexes with NSiN ligands is largely dominated by iridium where apart from the κ^3-(*Si*,*N*,*N*)-tridentate ligation, complexes with κ^2-

(*Si,N*)-bidentate and κ^1-(*Si*)-monodentate coordination mode have also been reported. The variation of the hapticity of the NSiN ligand from tridentate to monodentate in Ir-NSiN^A (NSiN^A = bis(8-quinolyl)methylsilyl) complexes has been associated with a high field shifting of the ^{29}Si resonances as observed in the ^{29}Si{^{1}H} NMR spectra of the respective compounds. A comparison between Ir-*fac*-κ^3-(*Si,N,N*)-NSiN complexes containing different NSiN ligands evidences that the silyl group at the bis(8-quinolyl)methylsilyl (NSiN^A) ligand exerts a stronger *trans* influence and *trans* effect than the respective silyl groups of bis(pyridine-2-yloxy)methylsilyl (NSiN^C) and bis-(4-methylpyridine-2-yloxy)methylsilyl (NSiN^D) ligands.

On the other hand, this review has revealed the state of the art on the catalytic applications of transition metal-NSiN complexes. Most of the contributions correspond to Ir-NSiN catalyzed processes although one example of a Rh-NSiN catalyst has also been found. It should be mentioned that most of the described mechanisms involve a Si-H hydrogen bond activation step as the rate determining step of the process. Others Ir-NSiN catalyzed processes which implicate CO_2 insertion into Si-N and Si-P bonds have also been described.

In summary, it could be concluded that the chemistry of transition metal complexes with monoanionic NSiN ligands as well as their catalytic applications are relatively underexplored. These ligands could contribute to the design of homogeneous catalysts *á la carte* due to the tunable character of the silyl group along with the donor ability of the nitrogen atoms. Therefore, it is expected that the future synthesis of new NSiN ligand precursors containing N-donor groups other than N-heterocycles, such as amines and/or anilines, could afford more active and reactive transition metal NSiN complexes.

Acknowledgements

Financial support from MINECO/FEDER project CTQ2015-67366-P and DGA/FSE group E07 is gratefully acknowledged. Dr. R. Lalrempuia acknowledged ARAID-Foundation for funding parts of this work.

References

[1] G. Rothenberg (Ed.), Catalysis: Concepts and Green Applications, Wiley-VCH, Weinheim, 2008.

[2] J. F. Hartwig, Organotransition Metal Chemistry: From Bonding to Catalysis, University Science Books, Sausalito, 2010.

[3] (a) G. van Koten, Pure Appl. Chem. 61 (1989), 1681-1694; (b) G. van Koten, D. Milstein (Eds.), Organometallic Pincer Chemistry, Topics in Organometallic Chemistry, Vol. 40, Springer, Heidelberg, 2013.

[4] D. Morales-Morales, C. M. Jensen (Eds.), The Chemistry of Pincer Compounds, Elsevier Science, Amsterdam, 2007.

[5] E. Peris, R. H. Crabtree, Coord. Chem. Rev. 248 (2004) 2239−2246.

[6] G. van Koten, R. A. Gossage (Eds.), The Privileged Pincer-Metal Platform: Coordination Chemistry and Applications, Topics in Organometallic Chemistry, Vol. 54, Springer, Heidelberg, 2016.

[7] For recent reviews, see: (a) S. Werkmeister, J. Neumann, K. Junge, M. Beller, Chem. Eur. J. 21 (2015) 12226-12250; (b) S. Chakraborty, P. Bhattacharya, H. Dai, H. Guan, Acc. Chem. Res. 48 (2015) 1995-2003; (c) C. Gunanathan, D. Milstein,

Chem. Rev. 114 (2014) 12024-12087; (d) H. A. Younus, N. Ahmad, W. Su, F. Verpoort, Coord. Chem. Rev. 276 (2014) 112-152; (e) M. E. O´Reilly, A. S. Veige, Chem. Soc. Rev. 43 (2014) 6325-6369; (f) J. Choi, A. H. Roy McArthur, M. Brookhart, A. S. Goldman, Chem. Rev. 111 (2011) 1761-1779.

[8] For a recent review on PSiP-complexes see: L. Turculet, PSiP Transition-Metal Pincer Complexes: Synthesis, Bond Activation, and Catalysis, of Pincer and Pincer-Type Complexes, Chapter 6, K. J. Szabó, O. F. Wendt (Eds.), Applications in Organic Synthesis and Catalysis, Wiley-VCH, Weinheim, 2014.

[9] For recent examples of ECE-complexes (E = Si^{II} and Ge^{II}) see: (a) A. Brück, D. Gallego, W. Wang, E. Irran, M. Driess, J. F. Hartwig, Angew. Chem. Int. Ed. 51 (2012) 11478-11482; (b) W. Wang, S. Inoue, E. Irran, M. Driess, Angew. Chem. Int. Ed. 51 (2012) 3691-3694.

[10] (a) R. Poli, Chem. Rev. 91 (1991) 509-511; (b) T. Cuenca, P. Royo, Coord. Chem. Rev. 193-195 (1999) 447-498; (c) B. Ye, N. Cramer, Acc. Chem. Res. 48 (2015) 1308-1318.

[11] (a) C. Slugovc, I. Padilla-Martínez, S. Sirol, E. Carmona, Coord. Chem. Rev. 213 (2001) 129–157; (b) C. Slugovc, R. Schmid, K. Kirchner, Coord. Chem. Rev. 185−186 (1999) 109–126.

[12] (a) B. J. Coe, S. J. Glenwright, Coord. Chem. Rev. 203 (2000) 5-80; (b) J. Zhu, Z. Lin, T. B. Marder, Inorg. Chem. 44 (2005) 9384-9390.

[13] (a) S. R. Stobart, X. Zhou, R. Cea-Olivares, A. Toscano, Organometallics 20 (2001) 4766−4768. (b) G. W. Bushnell, M. A. Casado, S. R. Stobart, Organometallics 20 (2001) 601−603; (c) X. Zhou, S. R. Stobart, Organometallics 20,

(2001) 1898−1900; (d) R. D. Brost, G. C. Bruce, F. L. Joslin, S. R. Stobart, Organometallics 16 (1997) 5669−5680; (e) X. Zhou, S. R. Stobart, R. A. Gossage, Inorg. Chem. 36 (1997) 3745−3749; (f) F. L. Joslin, S. R. Stobart, Inorg. Chem. 32 (1993) 2221-2223; (g) S. L. Grundy, R. D. Holmes-Smith, S. R. Stobart, M. A. Williams, Inorg. Chem. 30 (1991) 3333−3337; (h) F. L. Joslin, S. R. Stobart, J. Chem. Soc., Chem. Commun. (1989) 504−505.

[14] For recent examples of PSiP complexes see: (a) L. S. H. Dixon, A. F. Hill, A. Sinha, J. S. Ward, Organometallics 33 (2014) 653−658; (b) M. T. Whited, A. M. Deetz, J. W. Boerma, D. E. DeRosha, D. E. Janzen, Organometallics 33 (2014) 5070−5073; (c) M. J. Bernal, O. Torres, M. Martín, E. Sola, J. Am. Chem. Soc. 135 (2013) 19008−19015; (d) Y.-H. Li, X.-H. Ding, Y. Zhang, W.-R. He, W. Huang, Inorg. Chem. Commun. 15 (2012) 194−197; (e) Y.-H. Li, Y. Zhang, X.-H. Ding, Inorg. Chem. Commun. 14 (2011) 1306−1310; (f) H. Fang, Y.-K. Choe, Y. Li, S. Shimada, Chem. Asian J. 6 (2011) 2512-2521; (g) M. C. MacInnis, R. McDonald, M. J. Ferguson, S. Tobisch, L. Turculet, J. Am. Chem. Soc. 133 (2011) 13622−13633; (h) E. Sola, A. García-Camprubí, J. L. Andrés, M. Martín, P. Plou, J. Am. Chem. Soc. 132 (2010) 9111−9121; (i) A. García-Camprubí, M. Martín, E. Sola, Inorg. Chem. 49 (2010) 10649−10657; (j) S. J. Mitton, R. McDonald, L. Turculet, Angew. Chem., Int. Ed. 48 (2009) 8568−8571; (k) E. Morgan, D. F. MacLean, R. McDonald, L. Turculet, J. Am. Chem. Soc. 131 (2009) 14234−14236; (l) S. J. Mitton, R. McDonald, L. Turculet, Organometallics 28 (2009) 5122−5136; (m) D. F. MacLean, R. McDonald, M. J. Ferguson, A. J. Caddell, L. Turculet, Chem. Commun. (2008) 5146−5148; (n) E. E. Korshin, G. Leitus, L. J. W. Shimon, L. Konstantinovski, D. Milstein, Inorg. Chem. 47 (2008) 7177−7189; (o) M. C. MacInnis, D. F. MacLean, R. J. Lundgren, R. McDonald, L. Turculet, Organometallics 26 (2007) 6522−6525.

[15] (a) M. Stradiotto, K. L. Fujdala, T. D. Tilley, Chem. Commun. (2001) 1200–1201; (b) P. Sangtrirutnugul, T. D. Tilley, Organometallics 26 (2007) 5557–5568.

[16] (a) R. Lalrempuia, M. Iglesias, V. Polo, P. J. Sanz Miguel, F. J. Fernández-Alvarez, J. J. Pérez-Torrente, L. A. Oro, Angew. Chem. Int. Ed. 51 (2012) 12824-12827; (b) A. Julián, E. A. Jaseer, K. Garcés, F. J. Fernández-Alvarez, P. García-Orduña, F. J. Lahoz, L. A. Oro, Catal. Sci. Technol. 6 (2016) 4410-4417.

[17] P. Sangtrirutnugul, M. Stradiotto, T. D. Tilley, Organometallics 25 (2006) 1607–1617.

[18] K. Garcés, R. Lalrempuia, V. Polo, F. J. Fernández-Alvarez, P. García-Orduña, F. J. Lahoz, J. J. Pérez-Torrente, L. A. Oro, Chem. Eur. J. 22 (2016) 14717-14729.

[19] (a) P. Sangtrirutnugul, T. D. Tilley, Organometallics 27 (2008) 2223–2230; (b) S. Schwieger, R. Herzog, C. Wagner, D. Steinborn, J. Organomet. Chem. 694 (2009) 3548–3558; (c) C. A. M. Carr, C. W. Gribble, M. I. Gibson, Acta Cryst. E64 (2008) m472.

[20] W.-H. Kwok, G.-L. Lu, C. E. F. Rickard, W. R. Roper, L. J. Wright, J. Organomet. Chem. 689 (2004) 2511–2522.

[21] J. Yang, I. Del Rosal, M. Fasulo, P. Sangtrirutnugul, L. Maron, T. D. Tilley, Organometallics 29 (2010) 5544–5550.

[22] M. L. Buil, M. A. Esteruelas, I. Fernández, S. Izquierdo, E. Oñate, Organometallics 32 (2013) 2744−2752.

[23] (a) J. Sun, C. Ou, C. Wang, M. Uchiyama, L. Deng, Organometallics 34 (2015) 1546-1551; (b) J. Sun, L. Luo, Y. Luo, L. Deng, Angew. Chem. Int. Ed. 56 (2017) 2720-2724.

[24] A. J. Ruddy, S. J. Mitton, R. McDonald, L. Turculet, Chem. Commun. 48 (2012) 1159–1161.

[25] J. Yang, M. Fasulo, T. D. Tilley, New J. Chem. 34 (2010) 2528-2529.

[26] J. Yang, P. S. White, C. K. Schauer, M. Brookhart, Angew. Chem. Int. Ed. 47 (2008) 4141-4143.

[27] K. Garcés, F. J. Fernández-Alvarez, V. Polo, R. Lalrempuia, J. J. Pérez-Torrente, L. A. Oro, ChemCatChem 6 (2014) 1691-1697.

[28] (a) M. Safa, M. C. Jennings, R. J. Puddephatt, Chem. Commun. 46 (2010) 2811-2813; (b) M. Safa, M. C. Jennings, R. J. Puddephatt, Organometallics 31 (2012) 3539-3550.

[29] (a) B. Marciniec, C. Pietraszuk, Top. Organomet. Chem. 11 (2004) 197-248; (b) A. K. Roy, Adv. Organomet. Chem. 55 (2008) 1-59; (c) B. Marciniec, K. H. Maciejewski, C. Pietraszuk, P. Pawluć, Hydrosilylation: A Comprehensive Review on Recent Advances, B. Marciniec (Ed.), Springer, London, 2008.

[30] M. C. Lipke, A. L. Liberman-Martin, T. D. Tilley, Angew. Chem. Int. Ed. 56 (2017) 2260-2294.

[31] For some recent examples see: (a) Z. Yang, M. Zhong, X. Ma, K. Nijesh, S. De, P. Parameswaran, H. W. Roesky, J. Am. Chem. Soc. 138 (2016) 2548-2551; (b) Z. Yang, M. Zhong, X. Ma, S. De, C. Anusha, P. Parameswaran, H. W. Roesky, 54

(2015) 10225-10229; (c) T. J. Hadlington, M. Hermann, G. Frenking, C. Jones, J. Am. Chem. Soc. 136 (2014) 3028-3031.

[32] I. Ojima, The Hydrosilylation Reaction: The chemistry of Organosilicon Compounds, S. Patai, Z. Rappoport (Eds.), Wiley-VCH, New York, 1989.

[33] For earlier examples, see: (a) E. Frainnet, Pur. Appl. Chem. 19 (1969) 489-524; (b) E. Frainnet, V. Martel-Siegfried, E. Brousse, J. Dedier, J. Organomet. Chem. 85 (1975) 297–310; (c) I. Ojima, Y. Nagai, J. Organomet. Chem. 57 (1973) C42–C44; (d) E. Frainnet, R. Bourhis, J. Organomet. Chem. 93 (1975) 309–324; (e) I. Ojima, M. Nihonyanagi, T. Kogure, M. Kumagai, S. Horiuchi, K. Nakatsugawa, Y. Nagai, J. Organomet. Chem. 94 (1975) 449–461; (f) H. Sakurai, K. Miyoshi, Y. Nakadaira, Tetrahedron Lett. 18 (1977) 2671-2674.

[34] For recent examples, see and references there in: (a) C. Reyes, A. Prock, W. P. Giering, Organometallics 21 (2002) 546-554, (b) C. Thiot, A. Wagner, C. Mioskowski, Org. Lett. 8 (2006) 5939–5942; (c) S. K. U. Riederer, P. Gigler, M. P. Högerl, E. Herdtweck, B. Bechlars, W. A. Herrmann, F. E. Kühn, Organometallics 29 (2010) 5681–5692; (d) P. Gigler, B. Bechlars, W. A. Herrmann, F. E. Kühn, J. Am. Chem. Soc. 133 (2011) 1589-1596; (e) C. D. F. Königs, H. F. T. Klare, Y. Ohki, K. Tatsumi, M. Oestreich, Org. Lett. 14 (2012) 2842-2845.

[35] For some recent examples, see and references there in: (a) X. Liang, K. Wei, Y.-R. Yang, Chem. Commun. 51 (2015) 17471-17474; (b) M. Chen, J. F. Hartwig, J. Am. Chem. Soc. 137 (2015) 13972-13979; (c) H. Shen, J. Li, Q. Liu, J. Pan, R. Huang, Y. Xiong, J. Org. Chem. 80 (2015) 7212-7218; (d) T. Graening, J. F. Hartwig, J. Am. Chem. Soc. 127 (2005) 17192-17193.

[36] For a recent review, see: C. Cheng, J. F. Hartwig, Chem. Rev. 115 (2015) 8946-8975.

[37] (a) M. J. Fernández, P. M. Maitlis, Organometallics 2 (1983) 164-165; (b) M. J. Fernández, P. M. Maitlis, J. Chem. Soc., Dalton Trans. (1984) 2063-2066; (c) J. S. Ricci Jr., T. F. Koetzle, M. J. Fernández, P. M. Maitlis, J. C. Green, J. Organomet. Chem. 299 (1986) 383-389; (d) T. M. Gilbert, F. J. Hollander, R. G. Bergman, J. Am. Chem. Soc. 107 (1985) 3508-3516; (e) S. R. Klei, T. D. Tilley, R. G. Bergman, J. Am. Chem. Soc. 122 (2000) 1816-1817; (f) M. A. Esteruelas, F. J. Fernández-Alvarez, A. M. López, E. Oñate, P. Ruiz-Sánchez, Organometallics 25 (2006) 5131-5138.

[38] E. Gutiérrez-Puebla, A. Monge, M. Paneque, M. L. Poveda, S. Taboada, M. Trujillo, E. Carmona, J. Am. Chem. Soc. 121 (1999) 346-354.

[39] F. J. Fernández-Alvarez, A. M. Aitani, L. A. Oro, Cat. Sci. Technol. 4 (2014) 611-624.

[40] (a) E. A. Jaseer, M. N. Akhtar, M. Osman, A. Al-Shammari, H. B. Oladipo, K. Garcés, F. J. Fernández-Alvarez, S. Al-Khattaf, L. A. Oro, Cat. Sci. Technol. 5 (2015) 274-279; (b) H. B. Oladipo, E. A. Jaseer, A. Julián, F. J. Fernández-Alvarez, S. Al-Khattaf, L. A. Oro, J. CO_2 Utilization 12 (2015) 21-26.

[41] For some recent examples, see and references there in: (a) A. Tlili, E. Blondiaux, X. Frogneux, T. Cantat, Green Chem. 17 (2015) 157–168; (b) E. Blondiaux, J. Pouessel, T. Cantat, Angew. Chem. Int. Ed. 53 (2014) 12186–12190; (c) X. Frogneux, O. Jacquet, T. Cantat, Catal. Sci. Technol. 4 (2014) 1529–1533; (d) O. Jacquet, X. Frogneux, C. Das Neves Gomes, T. Cantat, Chem. Sci. 4 (2013) 2127-2131; (e) O. Jacquet, C. Das Neves Gomes, M. Ephritikhine, T. Cantat,

ChemCatChem 5 (2013) 117–120; (f) C. Das Neves Gomes, O. Jacquet, C. Villiers, P. Thuéry, M. Ephritikhine, T. Cantat, Angew. Chem. Int. Ed. 51 (2012) 187–190; (g) O. Jacquet, C. Das Neves Gomes, M. Ephritikhine, T. Cantat, J. Am. Chem. Soc. 134 (2012) 2934–2937.

[42] A. Julián, V. Polo, E. A. Jaseer, F. J. Fernández-Alvarez, L. A. Oro, ChemCatChem 7 (2015) 3895-3902.

[43] (a) E. W. Abel, I. H. Sabherwal, J. Chem. Soc. (A) (1968) 1105-1108; (b) H.-G. Horn, H. J. Lindner, Chem. Ztg. 112 (1988) 195-200; (c) R. Appel, B. Laubach, M. Siray, Tetrahedron Lett. 25 (1984) 4447-4448.

[44] K. Takeuchi, D. W. Stephan, Chem. Comm. 48 (2012) 11304-11306.

[45] (a) K. Diemert, T. Hahn, W. Kuchen, J. Organomet. Chem. 476 (1994) 173-181; (b) K. Diemert, T. Hahn, W. Kuchen, D. Mootz, W. Poll, P. Tommes, Z. Naturforsch. 50b (1995) 209-212.

[46] A. Julián, V. Polo, F. J. Fernández-Alvarez, L. A. Oro, Catal. Sci. Technol. 7 (2017) 1372-1378.

[47] For recent examples, see: (a) M. Aliaga-Lavrijsen, M. Iglesias, A. Cebollada, K. Garcés, N. García, P. J. Sanz Miguel, F. J. Fernández-Alvarez, J. J. Pérez-Torrente, L. A. Oro, Organometallics 34 (2015) 2378-2385; (b) M. Yu, H. Jing, X. Fu, Inorg. Chem. 52 (2013) 10741-10743; (c) W. Sattler, G. Parkin, J. Am. Chem. Soc. 134 (2012) 17462−17465; (d) A. Krüger, M. Albrecht, Chem. Eur. J. 18 (2012) 652−658; (e) Y. Kikukawa, Y. Kuroda, K. Yamaguchi, N. Mizuno, Angew Chem. Int. Ed. 51 (2012) 2434-2437; (f) A. Albright, R. E. Gawley, Tetrahedron Lett. 52 (2011) 6130−6132; (g) S. T. Tan, J. W. Kee, W. Y. Fan, Organometallics 30 (2011)

4008−4013; (h) T. Y. Lee, L. Dang, Z. Zhou, C. H. Yeung, Z. Lin, C. P. Lau, Eur. J. Inorg. Chem. (2010) 5675−5684.

[48] (a) W. Li, A. Wang, X. Yang, Y. Huang, T. Zhang, Chem. Commun. 48 (2012) 9183−9185; (b) J. John, E. Gravel, A. Hagège, H. Li, T. Gacoin, E. Doris, Angew. Chem. Int. Ed. 50 (2011) 7533−7536; (c) N. Asao, Y. Ishikawa, N. Hatakeyama, Menggenbateer, Y. Yamamoto, M. Chen, W. Zhang, A. Inoue, Angew. Chem. Int. Ed. 49 (2010) 10093−10095; (d) T. Mitsudome, S. Arita, H. Mori, T. Mizugaki, K. Jitsukawa, K. Kaneda, Angew. Chem. Int. Ed. 47 (2008) 7938−7940.

Graphical Abstract

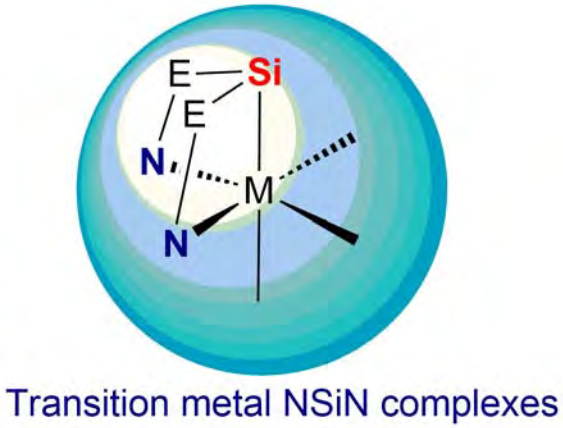

Text for the Graphical Abstract

Transition metal complexes with monoanionic NSiN-ligands and their applications in homogeneous catalysts.